

Synchronization of Complex Network Systems with Stochastic Disturbances

Kaihua Xi,^{*} Zhen Wang,[†] and Aijie Cheng[‡]

School of Mathematics, Shandong University, Jinan, Shandong, 250100, China

Hai Xiang Lin[§]

*Delft Institute of Applied Mathematics, Delft University of Technology, Delft, 2628 CD and
Institute of Environmental Sciences (CML), Leiden University, Leiden, 2333 CC, The Netherlands*

Jan H. van Schuppen[¶]

Delft Institute of Applied Mathematics, Delft University of Technology, Delft, 2628 CD, The Netherlands

Chenghui Zhang^{**}

School of Control Science and Engineering, Shandong University, Jinan, Shandong, 250061, China

We study the robustness of the synchronization of coupled phase oscillators. When fluctuations of phase differences in lines caused by disturbance exceed a certain threshold, the state cannot return to synchrony thus leading to desynchronization. Our main result is the deviation of explicit formulas of a variance matrix that characterizes the severity of these fluctuations. We highlight the utility of these results in two general problems: vulnerable line identification and network design. We find that the vulnerability of lines can be encoded by the cycle space of graphs. It is analytically shown that a line in large-size cycles is more vulnerable than those in small-size cycles and adding a new line or increasing coupling strength of a line reduces the vulnerability of the lines in any cycle including this line, while it does not affect the vulnerability of the other lines.

Synchronization of coupled phase oscillators has served as a paradigm for understanding collective behavior of real complex systems, where examples arise in nature (e.g., chimera spatiotemporal patterns [1], cardiac pacemaker cells[7]) and artificial systems (e.g., multi-agent systems[11], distributed optimization[23], power grids [13, 22], bridge oscillation [18]). If the synchronization is lost, the function of the system may be destroyed. Significant insights have been obtained from investigations on the emergence of a synchronous state, linear and non-linear stability and synchronization coherence. The synchronous state can be optimal subject to various criteria, e.g., critical coupling strength for the existence of a synchronous state [5, 6], linear stability [15], the value of an order parameter at a synchronous state [17], the volume of basin attraction around a stable synchronous state [3, 12] or the \mathcal{H}_2 norm of a linear system [16, 19]. The optimal condition can be achieved by redistributing the natural frequencies or network upgrading which includes rewiring the lines or changing coupling strength of lines. Of particular interest is to predict the behaviour of the network system when subjected to disturbances. If the fluctuations in the phase differences are so large that a synchronous state cannot be attained, then the synchronization is lost. Thus, the system may lose synchronization at the lines where the fluctuations in the phase difference are severe. Clearly, the risk of losing synchronization increases as the severity of the state fluctuation increases and, thus, the robustness decreases. We say a line is more vulnerable if the desynchronization occurs at this line more easily. In this Letter, we extend the investigations by asking how to assess the vulnerability of

lines in the network subjected to disturbances. With the answer of this question, we can pinpoint precisely to the effect of the disturbances on the vulnerability of lines and identify the vulnerable lines that may lead to desynchronization. In addition, the influences of network changes can also be evaluated. This provides a totally new and precise view to study the robustness of the systems.

For a graph $\mathcal{G} = (\mathcal{V}, \mathcal{E})$ with n nodes in \mathcal{V} and m lines in \mathcal{E} , we consider the dynamics of network-coupled phase oscillators governed by [9, 17, 21, 24]

$$\dot{\delta}_i = \omega_i + \sum_{j=1}^n l_{ij} \sin(\delta_j - \delta_i) \quad (1)$$

where δ_i is the phase of oscillator i ; ω_i is the natural frequency; l_{ij} is the coupling strength between nodes i and j and $l_{ij} > 0$ if nodes i and j are connected by a line, otherwise, $l_{ij} = 0$. When the non-linear term $\sin(\delta_j - \delta_i)$ is replaced by $(\delta_j - \delta_i)$, the model describes the consensus problem of multi-agent systems where the phases achieve a consensus. We focus on connected graphs, where $m \geq n - 1$ holds.

Here, we focus on the fluctuations in the phase differences in the lines around a synchronous state when subjected to stochastic disturbances. Without loss of generality, we assume $\sum_{i=1}^n \omega_i = 0$ and that there exists a synchronous state $\delta^* = \text{col}(\delta_i^*) \in \mathbb{R}^n$ such that $\delta_i^* \approx \delta_j^*$ for all the nodes and

$$\omega_i + \sum_{j=1}^n l_{ij} \sin(\delta_j^* - \delta_i^*) = 0,$$

which can be typically obtained by increasing the cou-

pling strength l_{ij} for all the lines. Since $\delta_i^* \approx \delta_j^*$, we obtain $\cos(\delta_j^* - \delta_i^*) \approx 1$. We focus on the following stochastic system, which is derived by linearization of the model (1),

$$\dot{\delta}_i = \sum_{j=1}^n a_{ij}(\delta_j - \delta_i) + b_i w_i, \quad (2)$$

where $a_{ij} = l_{ij}$, w_i is a Gaussian noise which models the disturbance, $b_i > 0$ is the strength of the disturbance. In system (2), the state variable $\delta_i(t)$ becomes the phase deviation from the synchronous state δ^* . To investigate the fluctuations of the phase differences around the synchronous state δ^* , we set the output of the system as

$$y_k = \delta_i - \delta_j, \quad (3)$$

where k is the index of line e_k connecting nodes i and j . The variance of the output y_k in its invariant probability distribution characterizes the severity of the phase difference in line e_k under stochastic disturbances. Thus it is a measure of the vulnerability of lines. In this Letter, we aim to derive the analytic expression of the variance matrix of the output, which reveals precisely the effects of the disturbances on the lines.

System (2) with output (3) is rewritten as

$$\dot{\boldsymbol{\delta}}(t) = -\mathbf{L}_a \boldsymbol{\delta}(t) + \mathbf{B} \mathbf{w}(t), \quad (4a)$$

$$\mathbf{y}(t) = \mathbf{C}^\top \boldsymbol{\delta}(t), \quad (4b)$$

where $\boldsymbol{\delta}(t) = \text{col}(\delta_i(t)) \in \mathbb{R}^n$ and $\mathbf{L}_a = (l_{a_{ij}}) \in \mathbb{R}^{n \times n}$ is the Laplacian matrix of the graph \mathcal{G} with weight a_{ij} for line (i, j) such that

$$l_{a_{ij}} = \begin{cases} -a_{ij}, & i \neq j, \\ -\sum_{k \neq i} l_{a_{ik}}, & i = j; \end{cases}$$

$\mathbf{B} = \text{diag}(b_i) \in \mathbb{R}^{n \times n}$; $\mathbf{w}(t) = \text{col}(w_i(t)) \in \mathbb{R}^n$; $\mathbf{y} = \text{col}(y_k) \in \mathbb{R}^m$ and $\mathbf{C} = (C_{ki}) \in \mathbb{R}^{m \times n}$ is the incidence matrix of graph \mathcal{G} such that

$$C_{ik} = \begin{cases} 1, & \text{if node } i \text{ is the begin of line } e_k, \\ -1, & \text{if node } i \text{ is the end of line } e_k, \\ 0, & \text{otherwise.} \end{cases}$$

where the direction of line e_k is arbitrarily specified and does not influence the investigation of the variances of the phase differences. The strength b_i of the disturbance at node i can be estimated by the standard process of system identification[10]. From the theory of complex network [2, 14], we obtain

$$\mathbf{C} \mathbf{R} \mathbf{C}^\top = \mathbf{L}_a$$

where $\mathbf{R} = \text{diag}(R_k) \in \mathbb{R}^{m \times m}$ with $R_k = a_{ij}$ being the weight of line e_k . Because the system (4) is linear, at any time, the probability distribution of the state is Gaussian.

For a linear Gaussian process where the system matrix is Hurwitz, the variance matrix of the output in the invariant probability distribution can be solved based on the controllability Gramian as defined in the **Appendix**. Here, a square matrix is called a Hurwitz matrix if every eigenvalue of this matrix has strictly negative real part. This variance matrix presents the variance of the output in the invariant probability distribution, i.e.,

$$\mathbf{Q}_\delta = \lim_{t \rightarrow \infty} E[\mathbf{y}(t) \mathbf{y}^\top(t)],$$

where $E[\cdot]$ denotes expectation of a random variable. The trace of \mathbf{Q}_δ is the \mathcal{H}_2 norm of the system (4) which is often used to study the performance of the synchronization of complex networks [16, 21].

Because \mathbf{L}_a is symmetric, there exists an orthogonal matrix $\mathbf{U} \in \mathbb{R}^{n \times n}$ such that

$$\mathbf{U}^\top \mathbf{L}_a \mathbf{U} = \boldsymbol{\Lambda}_n \quad (5)$$

where $\boldsymbol{\Lambda}_n = \text{diag}(\lambda_i) \in \mathbb{R}^{n \times n}$ with λ_i being the eigenvalue of matrix \mathbf{L}_a and $\lambda_1 = 0$. We decompose matrix $\mathbf{U} = [\mathbf{u}_1, \mathbf{U}_2]$ with $\mathbf{u}_1 = \tau \mathbf{1}_n$ and $\mathbf{U}_2 = [\mathbf{u}_2, \dots, \mathbf{u}_n] \in \mathbb{R}^{n \times (n-1)}$, where \mathbf{u}_i is the i -th column of \mathbf{U} and τ is a real number. Here, \mathbf{u}_i is the eigenvector corresponding to the eigenvalue λ_i of matrix \mathbf{L}_a . The variance matrix of the output \mathbf{y} is then obtained,

$$\mathbf{Q}_\delta = \mathbf{C}^\top \mathbf{U}_2 \mathbf{Q} \mathbf{U}_2^\top \mathbf{C}, \quad (6)$$

where $\mathbf{Q} = (q_{ij}) \in \mathbb{R}^{(n-1) \times (n-1)}$ satisfies

$$q_{ij} = (\lambda_{i+1} + \lambda_{j+1})^{-1} \mathbf{u}_{i+1}^\top \mathbf{B} \mathbf{B}^\top \mathbf{u}_{j+1}, \text{ for } i, j = 1, \dots, n-1. \quad (7)$$

In particular, the diagonal elements of \mathbf{Q} satisfy

$$q_{ii} = \frac{1}{2} \lambda_{i+1}^{-1} \mathbf{u}_{i+1}^\top \mathbf{B} \mathbf{B}^\top \mathbf{u}_{i+1} \text{ for } i = 1, \dots, n-1. \quad (8)$$

The diagonal elements of \mathbf{Q}_δ are the variances of the phase differences in the lines. Hence, vulnerable lines can be identified directly by the values of the diagonal elements, i.e., the line with the largest value is the most vulnerable. The effect of the network changes including adding new lines and increasing coupling strength of lines can be readily evaluated, which will be further explained in a following example. It follows from Eqs. (6-8) that if the eigenvalues of the Laplacian matrix \mathbf{L}_a decrease, the variances of the phase differences decrease; consequently, the robustness increases. This finding is consistent with the study by a perturbation method with a newly defined performance metric[21], where the robustness is related to the Kirchhoff indices.

Next, we use the formula on the networks with $b_i^2 = \beta$ for all the nodes, which leads to $\mathbf{B} \mathbf{B}^\top = \beta \mathbf{I}_n$, and investigate the effect of network changes on the variance of the

phase differences. We derive the explicit formula of the variance matrix for the networks,

$$\mathbf{Q}_\delta = \frac{\beta}{2} \mathbf{R}^{-1/2} \left(\mathbf{I}_m - \sum_{i=1}^{m-n+1} \mathbf{X}_i \mathbf{X}_i^\top \right) \mathbf{R}^{-1/2}, \quad (9)$$

where $\mathbf{I}_m \in \mathbb{R}^{m \times m}$ is an identity matrix and vector \mathbf{X}_i is the orthonormal basis of the kernel of $\mathbf{C}\mathbf{R}^{1/2}$, which can be calculated from the cycle space of the graph \mathcal{G} . The procedure to calculate \mathbf{X}_i is described in the **Appendix**.

Formula (9) reveals the role of the system parameters. The variance increases linearly with respect to the factor β . Because vector \mathbf{X}_i also depends on the weight a_{ij} of the lines, the relationship between the variance and the weight is nonlinear. Furthermore, formula (9) relates the robustness to the cycle space of graphs. This is the first time that this important relation is shown.

By means of this formula, we consider the variance in tree networks and show the effects of adding new lines and increasing the coupling strength of lines. We introduce two definitions for graphs, i.e., a *cycle-cluster* is a subgraph containing cycles which share at least one common line, and a *single line* is defined as a line that does not belong to any cycles. A line either belongs to a cycle-cluster or is a single line, and each pair of lines in a cycle-cluster are in at least one cycle. We introduce 3 networks with different topologies in the following example to explain our findings.

Example: Consider the 3 networks with 8 nodes shown in Fig. 1. The directions of the lines are arbitrarily specified, and the directions of all the cycles are chosen to be clockwise. These directions are set for the calculation of \mathbf{X}_i in formula (9) only, which does not mean the networks are directed. Networks (b) and (c) are constructed based on network (a) by adding lines e_8, e_9 and by adding lines e_8, e_9, e_{10} , respectively. The cycle-clusters and single lines of the networks are described in Table I. We set $b_i = 0.1$, $\mathbf{H}'(0) = 1$ for all the nodes in the 3 networks, which leads to $b_i^2 = \beta = 10^{-2}$ for all the nodes and $a_{ij} = l_{ij}$ for all lines.

Case 1: $\omega_i = 0$ for all the nodes and $l_{ij} = 1$ for all the lines in networks (a-c);

Case 2: $\omega_i = 0$ for all the nodes and $l_{ij} = 1$ for the lines $e_1 - e_9$ and $l_{14} = 2$ for e_{10} in network (c);

TABLE I. The cycle-clusters and single lines of the networks in Fig. 1.

Network	cycle-clusters	single lines
(a)	–	$e_1 - e_7$
(b)	$(e_2, e_3, e_4, e_9), (e_6, e_7, e_8)$	e_1, e_5
(c)	$(e_1, e_2, e_3, e_4, e_9, e_{10}), (e_6, e_7, e_8)$	e_5

The variances in the lines are shown in Table II. Here, the variances shown as fractions are calculated by

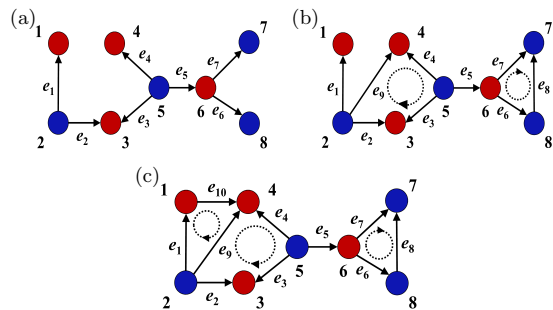


FIG. 1. Three networks with 8 nodes.

TABLE II. The diagonal elements of \mathbf{Q}_δ/β for the networks of Cases (1-2) in Fig 1.

Case	Net.	e_1	e_2	e_3	e_4	e_5	e_6	e_7	e_8	e_9	e_{10}
1	(a)	1/2	1/2	1/2	1/2	1/2	1/2	1/2	–	–	–
	(b)	1/2	3/8	3/8	3/8	1/2	1/3	1/3	1/3	3/8	–
	(c)	7/22	4/11	4/11	4/11	1/2	1/3	1/3	1/3	3/11	7/22
2	(c)	5/18	13/36	13/36	13/36	1/2	1/3	1/3	1/3	1/4	7/36
	(c*)	0.278	0.365	0.368	0.365	0.501	0.330	0.330	0.328	0.250	0.194

formula (9) following the procedure for computing the kernel of $\mathbf{C}\mathbf{R}^{1/2}$ in the **Appendix** and are verified by Matlab using formula (6). For example, the variances in the lines in network (a) can be calculated directly from $\frac{\beta}{2} \mathbf{R}^{-1}$ because the cycle space of a tree network is empty. In network (b), the bases of the kernel of the cycle space are $\xi_1 = [0, 0, 0, 0, 0, -1, 1, -1, 0]^\top$ and $\xi_2 = [0, -1, 1, -1, 0, 0, 0, 0, 1]^\top$, which are orthogonal. By scaling the vectors $\mathbf{R}^{-1/2} \xi_i$ for $i = 1, 2$ to unit length with $\mathbf{R} = \mathbf{I}_m$, we derive $\mathbf{X}_1 = [0, 0, 0, 0, 0, -1/\sqrt{3}, 1/\sqrt{3}, -1/\sqrt{3}, 0]^\top$ and $\mathbf{X}_2 = [0, -1/2, 1/2, -1/2, 0, 0, 0, 0, 1/2]^\top$. We obtain the variances of the phase differences using formula (9). In contrast, the decimal numbers in the last row with (c*) in the table are calculated from the simulations of system (4) for network (c) in Case 2. The simulation is conducted via the Euler-Maruyama method [8] with time $T = 10000$ and time step $dt = 10^{-3}$. Table II shows that the statistical values of the variances in the last row are very close to the analytical values for network (c) in Case 2. This verifies the correctness of formula (9).

The effects of adding new lines and increasing coupling strength are described next with the networks in Fig. 1. For the analytic derivation.

First, the variance of the phase difference in a single line connecting nodes i and j is $\frac{\beta}{2} a_{ij}^{-1}$. When considering the single lines shown in Table I, we find that the variances in these lines are all $\beta/2$, as shown in Table II. In addition, the variance in line e_5 is not affected by adding lines e_8, e_9 in network (b) or by adding lines e_8, e_9, e_{10} in network (c). Similarly, increasing the coupling strength of e_9 in network (c) in Case 2 also has no impact on this variance.

Second, adding new lines or increasing the coupling

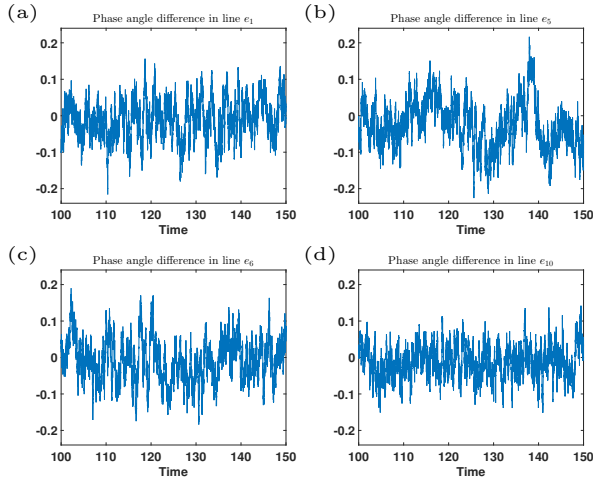


FIG. 2. Phase differences in 4 lines of network (c) in Case 2.

strength of lines in a cycle-cluster do not affect the variance of the phase differences in the lines outside this cycle-cluster. In network (c) of Case 1, the variances in lines e_6, e_7, e_8 are the same as those in network (b) and are not affected by adding of e_{10} . Similarly, in network (c) of Case 2, these variances are not changed by increasing the coupling strength of line e_{10} from 1 to 2 because line e_{10} is not in the cycle-cluster of (e_6, e_7, e_8) .

Third, by adding new lines or increasing the coupling strength of lines in a cycle-cluster, the variances of the phase differences in all the lines of this cycle-cluster will decrease. The calculation for networks (b-c) in Case 1 verify this finding, where the variances in lines e_2, e_3, e_4, e_9 decrease from $3\beta/8$ in network (b) to $4\beta/11, 4\beta/11, 4\beta/11$ and $3\beta/11$ in network (c), respectively, after adding line e_{10} . In addition, the variances further decrease to $13\beta/36, 13\beta/36, 13\beta/36$ and $\beta/4$ when the coupling strength of line e_{10} increases from 1 to 2 in network (c) in Case 2.

Fourth, for a cycle-cluster with only one cycle with lines in set \mathcal{E}_c in the graph, the variance of the phase difference in the line connecting nodes i and j is

$$\frac{\beta}{2} \left(a_{ij}^{-1} - a_{ij}^{-2} \left(\sum_{(r,q) \in \mathcal{E}_c} a_{rq}^{-1} \right)^{-1} \right). \quad (10)$$

In addition, if $a_{ij} = \gamma$ holds for all the lines, the variance becomes $\frac{\beta}{2\gamma} \left(1 - \frac{1}{N} \right)$, where N is the length of the cycle. In network (b) in Case 1, there are two cycles. By means of (10), it is obtained that the variances in lines e_6, e_7, e_8 are all $\beta/3$ and those in lines e_2, e_3, e_4, e_9 are all $3\beta/8$. This result demonstrates that forming small cycles can effectively suppress the variances of the phase differences. We conclude that formula (10) provides a conservative estimate of the variances in lines in cycle-clusters. In other words, the variance in a line that is in multiple cycles can be approximated by formula (10) by

considering the smallest cycle that includes this line. For example, the variance in line e_1 in network (c) in Case 1 can be approximated as $\beta/3$, which is calculated in the cycle (e_1, e_9, e_{10}) by formula (10) and is slightly larger than $7\beta/22$, as shown in Table II. Clearly, this value is conservative.

Finally, increasing the scale of the network will neither decrease nor increase the fluctuations of the phase differences; thus, it has no impact on the synchronization stability. This is a result from formula (9), where the variance matrix is determined by the strength of disturbance, the cycle space and the weights of the lines.

Regarding the vulnerability, we find that single lines are usually the most vulnerable. Fluctuations of the phase differences in lines e_1, e_5, e_6, e_{10} are illustrated in Fig. 2. It can be seen that the fluctuation in line e_5 is the most serious among these 4 lines while that in line e_{10} is the least serious. This finding is consistent with our analysis based on formula (9). We remark that for the networks with non-uniform disturbances, the lines with the most serious fluctuations can be identified by formula (6).

Formula (9) is derived in this letter with the assumption that the b_i values are identical for all the nodes in the network. Further study will focus on the deduction of the corresponding formulas without this assumption.

Appendix: The controllability Gramian

Consider a linear stochastic system,

$$\dot{\mathbf{x}}(t) = \mathbf{A}\mathbf{x}(t) + \mathbf{B}\boldsymbol{\mu}(t), \quad \mathbf{y} = \mathbf{C}\mathbf{x}(t),$$

where $\mathbf{x} \in \mathbb{R}^n$, $\mathbf{A} \in \mathbb{R}^{n \times n}$ is Hurwitz, $\mathbf{B} \in \mathbb{R}^{n \times n}$, $\mathbf{C} \in \mathbb{R}^{z \times n}$, the input is denoted by $\boldsymbol{\mu} \in \mathbb{R}^n$ and the output of the system is denoted by $\mathbf{y} \in \mathbb{R}^z$. The controllability Grammian of the pair (\mathbf{A}, \mathbf{B}) is defined as

$$\mathbf{Q}_x = \int_0^{+\infty} e^{\mathbf{A}t} \mathbf{B}\mathbf{B}^T e^{\mathbf{A}^T t} dt$$

which is the unique solution of the Lyapunov equation

$$\mathbf{A}\mathbf{Q}_x + \mathbf{Q}_x\mathbf{A}^T + \mathbf{B}\mathbf{B}^T = \mathbf{0}.$$

The variance matrix \mathbf{Q} of the output is $\mathbf{C}\mathbf{Q}_x\mathbf{C}^T$ [20].

Appendix: The cycle space of graphs

The cycle space of a graph is defined as the kernel of the incidence matrix \mathbf{C} , which is a vector subspace in \mathbb{R}^m . Because $\text{rank}(\mathbf{C}) = n - 1$, the dimension of the cycle space is $m - n + 1$. Considering a cycle \mathcal{C} with set \mathcal{E}_c of lines in the graph \mathcal{G} , we specify a direction for \mathcal{C} ; then, the

vector $\xi_c = [\xi_{c_1}, \xi_{c_2}, \dots, \xi_{c_m}]^\top \in \mathbb{R}^m$ such that

$$\xi_{c_k} = \begin{cases} +1, & \text{if } e_k \in \mathcal{E}_c \text{ with direction} = \text{the cycle direction,} \\ -1, & \text{if } e_k \in \mathcal{E}_c \text{ with direction} \neq \text{the cycle direction,} \\ 0, & \text{otherwise,} \end{cases}$$

belongs to the kernel of \mathbf{C} such that $\mathbf{C}\xi_c = \mathbf{0}$ [2]. The basis vectors for the cycle space can be derived by taking the vectors as ξ_c corresponding to the $(m - n + 1)$ *fundamental cycles* [4] in the graph. Because \mathbf{R} is non-singular, the vectors $\mathbf{R}^{-1/2}\xi_c$ for all the cycles are basis vectors of the kernel of $\mathbf{C}\mathbf{R}^{1/2}$. The orthonormal basis vectors \mathbf{X}_i are obtained via Gram-Schmidt orthogonalization of the basis vectors $\mathbf{R}^{-1/2}\xi_c$.

* kxi@sdu.edu.cn

† wangzhen17@mail.sdu.edu.cn

‡ aijie@sdu.edu.cn

§ H.X.Lin@tudelft.nl

¶ jan.h.van.schuppen@xs4all.nl

** zchui@sdu.edu.cn

- [1] D. M. Abrams and S. H. Strogatz. Chimera states for coupled oscillators. *Phys. Rev. Lett.*, 93:174102, 2004.
- [2] N. Biggs. *Algebraic Graph Theory*. Cambridge University Press, 2nd edition, 1993.
- [3] R. Delabays, M. Tyloo, and Ph. Jacquod. The size of the sync basin revisited. *Chaos*, 27(10):103109, 2017.
- [4] R. Diestel. *Graph Theory*. Springer-Verlag, New York 1997, 2000.
- [5] F. Dörfler and F. Bullo. Synchronization in complex networks of phase oscillators: A survey. *Automatica*, 50(6):1539 – 1564, 2014.
- [6] M. Fazlyab, F. Dörfler, and V. M. Preciado. Optimal network design for synchronization of coupled oscillators. *Automatica*, 84:181 – 189, 2017.
- [7] L. Glass and M. C. Mackey. *From Clocks to Chaos: The Rhythms of Life*. Princeton University Press, Princeton, NJ, 1988.
- [8] D. J. Higham. An algorithmic introduction to numerical simulation of stochastic differential equations. *SIAM Rev.*, 43:525–546, 2001.
- [9] Y. Kuramoto. Self-entrainment of a population of coupled non-linear oscillators. In *International Symposium on Mathematical Problems in Theoretical Physics*, pages 420–422. Springer Berlin Heidelberg, 1975.
- [10] L. Ljung. *System Identification: Theory for the User*. Prentice Hall PTR, 1999.
- [11] C. Ma and J. Zhang. Necessary and sufficient conditions for consensusability of linear multi-agent systems. *IEEE Trans. Autom. Control*, 55(5):1263–1268, 2010.
- [12] P. J. Menck, J. Heitzig, N. Marwan, and Jürgen Kurths. How basin stability complements the linear-stability paradigm. *Nat. Phys.*, 9(2):89–92, jan 2013.
- [13] A. E. Motter, S. A. Myers, M. Anghel, and T. Nishikawa. Spontaneous synchrony in power-grid networks. *Nat. Phys.*, 9(3):191–197, feb 2013.
- [14] P. Van Mieghem. *Graph spectra of complex networks*. Cambridge university press, 2008.
- [15] Louis M. Pecora and Thomas L. Carroll. Master stability functions for synchronized coupled systems. *Phys. Rev. Lett.*, 80:2109–2112, Mar 1998.
- [16] B. K. Poolla, S. Bolognani, and F. Dörfler. Optimal placement of virtual inertia in power grids. *IEEE Trans. Autom. Control*, 62(12):6209–6220, 2017.
- [17] Per Sebastian Skardal, Dane Taylor, and Jie Sun. Optimal synchronization of complex networks. *Phys. Rev. Lett.*, 113:144101, Sep 2014.
- [18] S. Strogatz, D. Abrams, and A. McRobie et al. Crowd synchrony on the millennium bridge. *Nature*, page 43–44, 2005.
- [19] E. Tegling, B. Bamieh, and D. F. Gayme. The price of synchrony: Evaluating the resistive losses in synchronizing power networks. *IEEE Trans. Control Netw. Syst.*, 2(3):254–266, Sept 2015.
- [20] R. Toscano. *Structured controllers for uncertain systems*. Springer-verlag, London, 2013.
- [21] M. Tyloo, T. Coletta, and Ph. Jacquod. Robustness of synchrony in complex networks and generalized kirchhoff indices. *Phys. Rev. Lett.*, 120:084101, Feb 2018.
- [22] K. Xi, J. L. A. Dubbeldam, and H. X. Lin. Synchronization of cyclic power grids: equilibria and stability of the synchronous state. *Chaos*, 27(1):013109, 2017.
- [23] Tao Yang, Xinlei Yi, Junfeng Wu, Ye Yuan, Di Wu, Ziyang Meng, Yiguang Hong, Hong Wang, Zongli Lin, and Karl H. Johansson. A survey of distributed optimization. *Annual Reviews in Control*, 47:278–305, 2019.
- [24] Xiyun Zhang, Stefano Boccaletti, Shuguang Guan, and Zonghua Liu. Explosive synchronization in adaptive and multilayer networks. *Phys. Rev. Lett.*, 114:038701, Jan 2015.